

## FINITE AMPLITUDE ONE-DIMENSIONAL WAVE PROPAGATION IN A THERMOELASTIC HALF-SPACE

J. ABOUDI†

Department of Mathematics, University of Strathclyde, Glasgow, Scotland  
and

Y. BENVENISTE

School of Engineering, Tel-Aviv University, Ramat Aviv, Israel

(Received 5 March 1973; revised 24 May 1973)

**Abstract**—The problem of finite wave propagation in a nonlinearly thermoelastic half-space is considered. The surface of the half-space is subjected to a time-dependent thermal and normal mechanical loading. The solution is obtained by a numerical procedure, which is shown to furnish accurate results, and linear dynamic thermoelastic problems are obtained as special cases. The accuracy of the results is checked by comparison with some known analytical solutions which can be obtained in some special cases of both the linear and the nonlinear problems. In those cases where the solution contains shocks, it is shown that the numerical results satisfy the necessary jumps conditions which need to hold across such discontinuities.

### INTRODUCTION

In the last years several works investigating the propagation of finite amplitude waves in materials with nonlinear constitutive equations have been published. The majority of the work done in this area neglects the effect of heat conduction. In spite of this basic assumption, the governing equations being nonlinear are still difficult to treat and analytic solutions have been found only under restrictive boundary conditions as in the works by Chu[1] and Collins[2]. Others have used the method of wave front expansion and obtained solutions valid only for short times after the arrival of the wave front, see for example Reddy and Achenbach[3], Achenbach and Reddy[4], Lubliner and Green[5] and Vogt and Schapery[6]. In order to find solutions under arbitrary time dependent loadings and which are valid for all times, the authors have used a numerical method, see Aboudi and Benveniste[7]. In [7] the problem of nonlinearly elastic half-space subjected to combined normal and shear loadings is solved, shock formation and propagation are successfully treated, and the numerical method is shown to yield accurate results by comparison with analytical conclusions which could be drawn under special boundary conditions.

When the effect of heat conduction is taken into account, the governing equations are of mixed hyperbolic–parabolic type and the class of analytical solutions which could be found are much more restricted. Even in the linear theory of thermoelasticity substantial difficulties are encountered in obtaining closed form solutions to the complete coupled system of equations, and usually only solutions valid for small times are obtained, see for example, Boley and Tolins[8] and Soler and Brull[9]. When finite wave propagation in

† On leave from School of Engineering, Tel-Aviv University, Ramat Aviv, Israel.

heat conducting materials is considered, the equations become more complicated due to their nonlinear nature. To our knowledge the only existing analytical solutions to the complete equations including thermal terms in nonlinear dynamic elasticity are the dilatational constant profile given by Bland[10] and the quasi-transverse constant profile discussed by Craine[11].

In the first part of this work a numerical procedure to solve the problem of finite amplitude wave propagation in a nonlinearly conducting elastic half-space with arbitrarily normal time-dependent loading is described.

In the linear thermoelastic problems this scheme is checked in some special cases where analytical solutions are available as those given by Sternberg and Chakravorty[12] for the non coupled problem, and by Dillon[13] when the coupling parameter equals unity.

In the nonlinear problems we chose as a matter of convenience a quadratic material[10], and Newton's law of heat conduction is adopted. The accuracy of the obtained numerical results is confirmed by the following checks. (1) For small displacement gradient boundary inputs, the numerical solution of the nonlinear thermoelastic problem reduces to the solution of the linear problem. (2) The half-space is subjected to a monotonically decreasing normal loading. By equating the conductivity to zero, the solution of the purely mechanical problem, which has a simple wave analytical solution[7], is numerically obtained. The agreement between the two solutions is excellent. (3) A constant wave profile representing a rigidly propagating wave is produced. Such a solution is obtained only when a certain special profile is imposed on the boundary as a boundary condition. As a matter of convenience in order to have a closed form analytic expression for such a profile, a special material given in [10] is chosen only for this check. When this solution is imposed on the boundary, the numerical scheme produces the rigidly propagating wave form at any point inside the half-space. (4) The boundary is subjected to a step input in the displacement gradient, and at points inside the half-space it is shown that across the obtained shocks the Rankine-Hugoniot equations and the second law of the thermodynamics are satisfied. This important check confirms that the shocks are successfully treated.

#### STATEMENT OF THE PROBLEM

Consider a quadratic material for which the specific energy is given in a non-dimensional form by [10].

$$U = T_1 S + 0.5\lambda I_1^2/\rho + \mu I_2/\rho - KI_1 S + 0.5\eta S^2 \quad (1)$$

where  $T_1$  is the base temperature at which the material is undisturbed,  $S$  is the specific entropy,  $I_1$  and  $I_2$  are the first and second invariants of the Green strain tensor as defined in [10],  $\rho$  is the density of the undeformed state and  $\lambda$ ,  $\mu$ ,  $K$ ,  $\eta$  are material constants.

Considering the one-dimensional motion of a half-space in which only one displacement  $u$  in the depth direction exists, the above expression for  $U$  reduces to:

$$U = T_1 S + 0.5\phi(m + 0.5m^2)^2 - KS(m + 0.5m^2) + 0.5\eta S^2 \quad (2)$$

where

$$m = \frac{\partial u}{\partial a} \quad \text{and} \quad \phi = (\lambda + 2\mu)/\rho$$

with  $a$  describing the non-dimensional coordinate of the particle in the undeformed state and  $u$  is the non-zero displacement component.

The dimensional quantities (with caret) are given by

$$\hat{U} = U\hat{c}_0^2, \quad \hat{S} = \hat{c}_0^2 S/\hat{T}_0, \quad \hat{\rho} = \hat{\rho}_0 \rho, \quad \hat{T} = \hat{T}_0 T, \quad \hat{a} = \hat{a}_0 a$$

where we introduced the reference units  $\hat{c}_0$ ,  $\hat{T}_0$ ,  $\hat{\rho}_0$  and  $\hat{a}_0$  for the velocity, temperature, density and length respectively. In the sequel  $\hat{T}_0$  will be chosen to be the basic temperature  $\hat{T}_1$ ,  $\hat{\rho}_0$  to be the density of the undeformed state  $\hat{\rho}$  and  $\hat{c}_0$  to be the quantity  $[(\hat{\lambda} + 2\hat{\mu})/\hat{\rho}]^{1/2}$ .  $\hat{\lambda}$ ,  $\hat{\mu}$ ,  $\hat{K}$  and  $\hat{\eta}$  are related to their non-dimensional quantities according to:

$$\hat{\lambda} = \hat{c}_0^2 \hat{\rho}_0 \lambda; \quad \hat{\mu} = \hat{c}_0^2 \hat{\rho}_0 \mu, \quad \hat{K} = K\hat{T}_0, \quad \hat{\eta} = \eta\hat{T}_0^2/\hat{c}_0^2.$$

The equations of motion and heat conduction in the absence of body forces and thermal sources in the Lagrangian description are given in the present one-dimensional case by:

$$\left. \begin{aligned} \frac{\partial^2 u}{\partial t^2} &= \frac{\partial}{\partial a} \left( \frac{\partial U}{\partial m} \right) \\ \rho T \frac{\partial S}{\partial t} &= - \frac{\partial Q}{\partial a} \end{aligned} \right\} \tag{3}$$

where the temperature  $T$  is given by:

$$T = \frac{\partial U}{\partial S} = T_1 + \eta S - K(m + 0.5m^2) \tag{4}$$

and the Lagrangian heat flux  $Q$  given by:

$$Q = -k \frac{\partial T}{\partial a} \tag{5}$$

where  $k$  is the coefficient of heat conduction (assuming it is constant) and  $t$  is the time. The dimensional time, heat flux and heat conductivity are given respectively by:

$$\hat{t} = \hat{a}_0 t/\hat{c}_0, \quad \hat{Q} = \hat{c}_0^3 \hat{\rho}_0 Q, \quad \hat{k} = k\hat{c}_0^3 \hat{\rho}_0 \hat{a}_0/\hat{T}_0.$$

With  $U$  given by equation (2) we obtain in terms of the displacement and the temperature and their derivatives the following equations of motion and heat conduction

$$\frac{\partial^2 u}{\partial t^2} = \frac{\partial^2 u}{\partial a^2} \left[ \left\{ 1.5 \left( \frac{\partial u}{\partial a} \right)^2 + 3 \frac{\partial u}{\partial a} + 1 \right\} (\phi - K^2/\eta) - K(T - T_1)/\eta \right] - \frac{K}{\eta} \left( 1 + \frac{\partial u}{\partial a} \right) \frac{\partial T}{\partial a} \tag{6}$$

$$T \frac{\partial T}{\partial t} = \frac{k\eta}{\rho} \frac{\partial^2 T}{\partial a^2} - KT \frac{\partial^2 u}{\partial a \partial t} \left( 1 + \frac{\partial u}{\partial a} \right). \tag{7}$$

For  $t \leq 0$  the half-space  $a \geq 0$  is undisturbed ( $u = 0, T = T_1$ ) and at  $t > 0$  it is set in motion by applying time dependent thermal and mechanical disturbances at  $a = 0$ . Thus:

$$\left. \begin{aligned} u(a, t) &= 0 \\ \frac{\partial u}{\partial t} &= 0 \\ T(a, t) &= T_1 \end{aligned} \right\} t \leq 0 \tag{8}$$

and

$$m(0, t) = f(t) \quad (9)$$

$$T(0, t) = T_1 + g(t) \quad (10)$$

where  $f(t)$ ,  $g(t)$  are prescribed time functions.

The system of equations (6–7) together with the initial boundary conditions (8–10) and the boundedness of the displacement and temperature as  $a \rightarrow \infty$  govern completely the motion at  $t > 0$ . This system is known to be of the mixed hyperbolic–parabolic type. The parabolic part is present due to the inclusion of heat conduction which is the main aim of this paper.

#### NUMERICAL SOLUTION

In the following we propose a finite-difference solution to the mixed system (6–7) together with its initial and boundary conditions. By comparing the obtained numerical results with some special cases in which some analytical conclusions could be drawn, it will be shown that the numerical procedure yields reliable accuracy.

Let us introduce a space division of intervals  $\Delta a$  and time increments  $\Delta t$ . Similar to [7], equation (6) is solved by an explicit approximation which yields the displacement at the time level  $t + \Delta t$  in terms of the already known displacements and temperature at time  $t$  and  $t - \Delta t$  as follows:

$$u_i^{n+1} = 2u_i^n - u_i^{n-1} + (\Delta t)^2 L[u_i^n, T_i^n] \quad (11)$$

where

$$u_i^n = u(i \Delta a, n \Delta t),$$

$$T_i^n = T(i \Delta a, n \Delta t),$$

$$i = 0, 1, 2, \dots$$

$$n = 2, 3, 4, \dots$$

and  $L$  is a spatial difference operator which expresses the discretized version of the differential expression on the right hand side of (6). The discretization is obtained by approximating all the derivatives by their corresponding central difference versions which are correct up to second order in  $\Delta a$ . For the grid point at the boundary  $a = 0$ , an additional auxiliary point is introduced at  $a = -\Delta a$  such that the value of the displacement at this point is computed according to the boundary condition (9) as follows:

$$u_{-1}^n = u_0^n - \Delta a f(t). \quad (12)$$

On the other hand the derivative of the temperature  $\partial T / \partial a$  in (6) at  $a = 0$  is computed according to the following approximation:

$$\frac{\partial T}{\partial a} = [-1.5T_0^n + 2T_1^n - 0.5T_2^n] / \Delta a + O(\Delta a^2). \quad (13)$$

For the temperature equation (7), an implicit finite-difference scheme must be employed in order to prevent the need of considerably small time increments  $\Delta t$  known to be required when approximating a parabolic equation such as (7) by a simple explicit scheme.

We choose here for (7) the Crank–Nicolson implicit scheme[14] which yields the following system of algebraic equations:

$$-\varepsilon T_{i-1}^{n+1} + (2\varepsilon + T_i^n)T_i^{n+1} - \varepsilon T_{i+1}^{n+1} = \varepsilon(T_{i+1}^n + T_{i-1}^n) + T_i^n(T_i^n - 2\varepsilon - \Delta t p_i^n) \quad i = 1, 2, \dots, N \quad (14)$$

where:

$$\varepsilon = k\eta \Delta t / 2\rho(\Delta a)^2$$

$$p_i^n = K(1 + \bar{m}_i^n)\bar{m}_i^n$$

and  $\bar{m}_i^n$ ,  $\bar{m}_i^n$  are the central difference approximations of  $\partial u / \partial a$ ,  $\partial^2 u / \partial a \partial t$  respectively.

Equations (14) form a system of  $N$  algebraic equations in the unknowns  $T_i^{n+1}$  ( $i = 1, 2, \dots, N$ ) where  $N = a_1 / \Delta a$  with  $a_1$  being a point within the half-space at which the values of the displacement and temperature have no influence (for a preassigned degree of accuracy) on their values at smaller distances  $a < N \Delta a$  for given ranges of space and time. Accordingly we can substitute zero for the various quantities at  $i = N + 1$  for every time  $t$  within the mentioned time and space ranges. In (14)  $T_0^{n+1}$  is determined according to the boundary condition (10).

It is obvious from (14) that at every time step, a system of equations of a tridiagonal matrix is to be solved in order to obtain the temperature at the various grid points within the half-space. Such a solution can be easily obtained by a direct Gauss elimination[14].

The present proposed difference scheme (11–14) is found satisfactory and accurate whenever it is applied to problems possessing a smooth solution. On the other hand when it is applied to problems which have a discontinuous solution, such as those containing shock waves, numerical oscillations which are quite strong are formed which may in time distort the true solution, see also [7] for more detailed discussion.

In order to remove these oscillations, an iterative process previously employed in [7] is applied on the explicit scheme (11) as follows:

$$u_i^{n+1, j} = 2u_i^n + u_i^{n-1} + (\Delta t)^2 \{w_3 L[u_i^{n+1, j-1}, T_i^n] + w_2 L[u_i^n, T_i^n] + w_1 L[u_i^{n-1}, T_i^{n-1}]\} / (w_1 + w_2 + w_3) \quad j = 1, 2, \dots \quad (15)$$

where  $u_i^{n+1, 0}$  is defined to be equal to  $u_i^{n+1}$  given by (11),  $w_i$  are weight numbers and  $j$  is the number of iterations. Actual computations with (11–15) show that one iteration only ( $j = 1$ ) removes almost all the oscillations near the shock. Accordingly all the results given in this paper are obtained by applying one iteration only.

The difference scheme (14) is an implicit one, therefore in the linear case it is stable for every value of the time increment. On the other hand the scheme (11), (15) is explicit and a stability condition is needed which imposes a limitation on the range of possible values that  $\Delta t$  can attain for a given  $\Delta a$ . We found experimentally that such a condition is within the range of the stability criterion of the corresponding purely mechanical problem as previously developed in [7].

The coefficients  $w_i$  which appear in (15) need to satisfy the restrictions of the stability condition, and moreover, they have to be chosen in such a way that the scheme yields the best possible results in the sense that numerical oscillation amplitudes near the shocks are minimized, and produces in the test cases the analytically expected results. Accordingly we found that  $w_1 = -1$ ,  $w_2 = 10$ ,  $w_3 = 0$  furnish the best results.

All the results in this paper are given for the mesh space increment  $\Delta a = 0.01$ , and the system of equations (14) was solved for  $N = 400$ , where for the observation points at  $0 < a < 0.5$  and the time interval  $0 < t < 1$ , the values of the displacement and temperature at  $a_1 = 4$  were actually negligible.

In this paper we chose  $\mu = 1/3$ ,  $\lambda = 1/3$  and  $K = 1$ . The parameter  $\eta$  must satisfy the inequality, Bland[10],

$$\eta > \rho K^2 / (\lambda + \frac{2}{3}\mu).$$

We chose  $\eta = 2$  which obviously satisfies this condition. Finally whenever unstated otherwise the coefficient of conductivity is  $k = 1$ .

LINEAR THERMOELASTICITY

Although our main aim is to solve the nonlinear thermoelastic problem, we start here with the linear theory for which there exist in some certain cases simple analytical solutions which serve as a check for our numerical scheme in the linear case.

Consider a long thin rod in which the only nonzero stress component is the axial one. Then the linearized thermoelastic equations of motion are given according to Dillon[13] in a non-dimensional form by:

$$\left. \begin{aligned} \frac{\partial^2 u}{\partial t^2} &= \frac{\partial^2 u}{\partial x^2} - \frac{\partial T}{\partial x} \\ (1 - \delta) \frac{\partial T}{\partial t} &= \frac{\partial^2 T}{\partial x^2} - \delta \frac{\partial^2 u}{\partial x \partial t} \end{aligned} \right\} \tag{16}$$

where  $u$  is the displacement in the axial direction  $x$  and  $\delta$  is the thermoelastic coupling parameter, see [13] for details.

In the special case of the uncoupled equations ( $\delta = 0$ ) and with the boundary conditions

$$\text{and } \left. \begin{aligned} \frac{\partial u}{\partial x} - T &= 0 \\ T(x, t) &= H(t) \end{aligned} \right\} \text{ at } x = 0 \tag{17}$$

where  $H(t)$  is the Heaviside step function, the solution of (16) is given by [12]:

$$T(x, t) = \psi(\theta_1) = \text{erfc}(\theta_1), \quad \theta_1 = x/2t^{1/2}, \quad t > 0 \tag{18}$$

and

$$u(x, t) = H(t - x)[1 - \exp(t - x)] + x\psi(\theta_1) - 2(t/\pi)^{1/2} \exp(-\theta_1^2) + 0.5\beta(x, t) \tag{19}$$

where

$$\beta(x, t) = \exp(t - x)\psi(\theta_1 - t^{1/2}) - \exp(t + x)\psi(\theta_1 + t^{1/2})$$

and  $\text{erfc}(\theta_1)$  is the complementary error function.

The corresponding difference schemes of (16) together with the appropriate boundary conditions (17) are similar to those given by (11, 14, 15) but more easier.

In Fig. 1 the analytical solutions (18-19) for  $\partial u/\partial x$  and  $T$  are shown together with the corresponding numerical ones at the observation point  $x = 0.5$ . It is well seen that at the

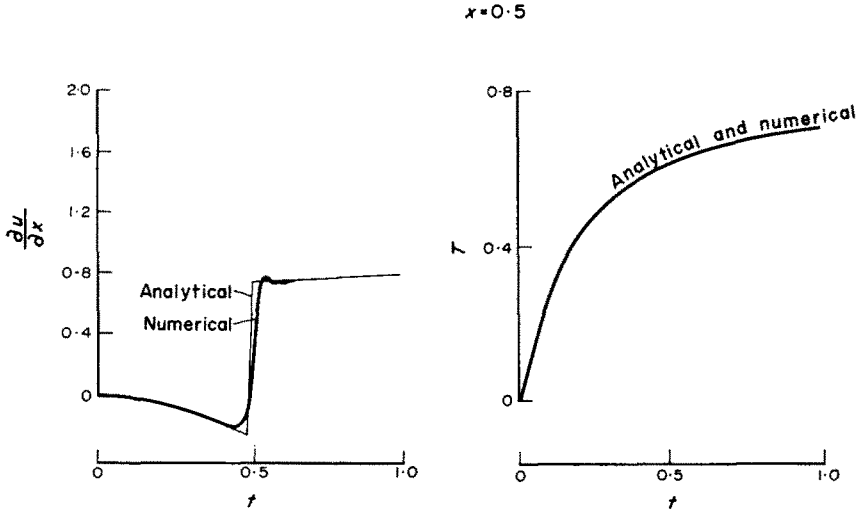


Fig. 1. Analytical and numerical solutions of the linear thermoelastic problem (16), (17) with  $\delta = 0$  for the displacement gradient and temperature are shown at the observation point  $x = 0.5$ . The two solutions for the temperature coincide.

smooth parts of the solutions very good correspondence between the two solutions is obtained (for example, the two solutions for the temperature  $T$  are indistinguishable). In the steep part of  $\partial u/\partial x$ , the numerical solution shows a slightly smeared step, but it still yields the correct jump in the displacement gradient.

A different problem for which a simple analytical solution exists is given by Dillon[13]. In [13] a solution to the thermoelastic equations (16) is derived for the special case of the coupling parameter equal unity ( $\delta = 1$ ), with the boundary conditions:

$$\text{and } \left. \begin{aligned} u(x, t) &= V_0 t H(t) \\ \frac{\partial T}{\partial x} &= 0 \end{aligned} \right\} \text{ at } x = 0. \tag{20}$$

The solution for the displacement gradient is given by

$$\frac{\partial u}{\partial x} = -V_0 \exp(-t/2) I_0[0.5(t^2 - x^2)^{1/2}] H(t - x) \tag{21}$$

where  $I_0$  is the modified Bessel function of order zero. The solution for the corresponding uncoupled problem ( $\delta = 0$ ) is

$$\frac{\partial u}{\partial x} = -V_0 H(t - x). \tag{22}$$

In Figs. 2(a) and 2(b) the two analytical solutions (21) and (22), respectively, are shown (for  $V_0 = 1$ ), together with the corresponding numerical ones. Here also good correspondence between the two methods is obtained. In Fig. 2(c) the numerical solution for the coupled case with ( $\delta = \frac{1}{2}$ ) is shown for comparison.

We conclude therefore that the proposed finite-difference scheme described previously yields good results in the present case of linear thermoelastic problems. In the next sections we shall examine it for the more complicated case of nonlinear thermoelasticity.

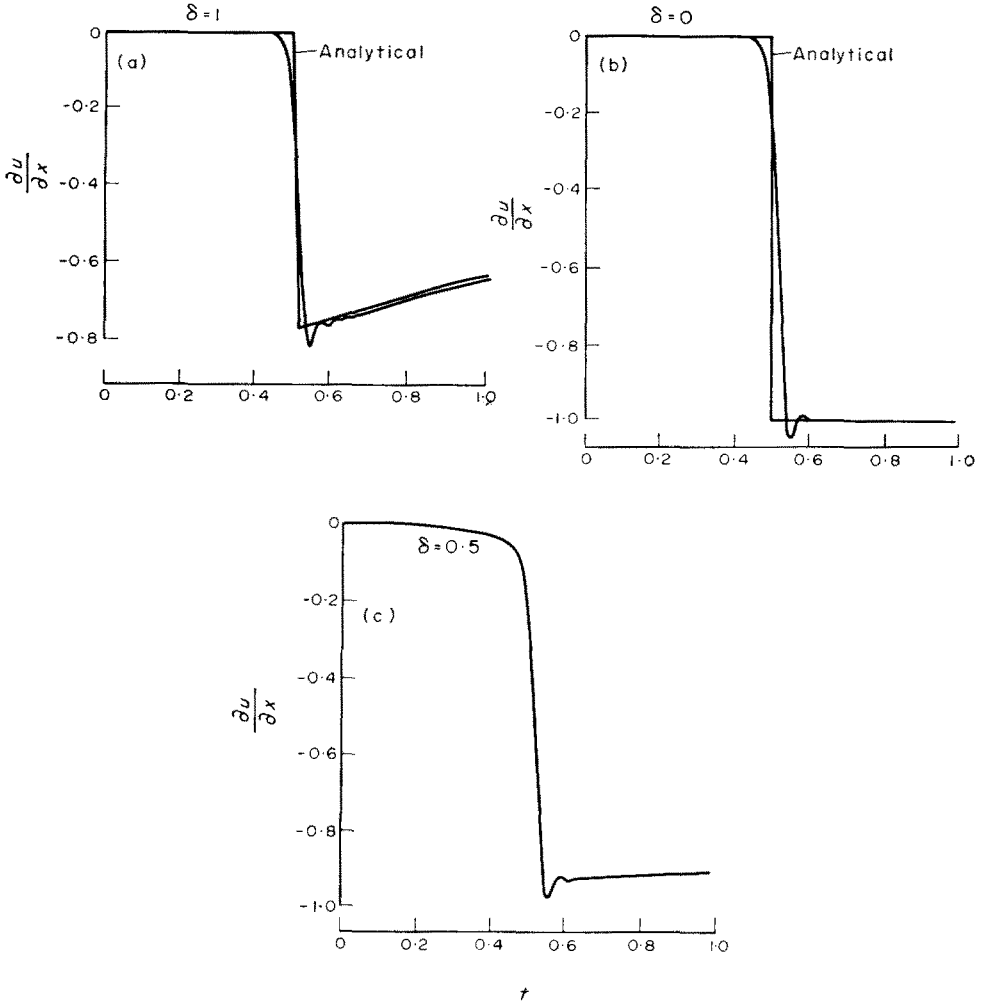


Fig. 2. (a) Analytical and numerical solutions of the linear thermoelastic problem (16), (20) with  $\delta = 1$  for the displacement gradient are shown at  $x = 0.5$ . (b) Same as (a) for  $\delta = 0$ . (c) Numerical solution of (16), (20) with  $\delta = \frac{1}{2}$  for the displacement gradient at  $x = 0.5$ .

NON-LINEAR THERMOELASTICITY

In the present section we use the complete numerical scheme (11-14) in order to handle the problem of one-dimensional wave propagation in a nonlinearly elastic conducting half-space.

As a first check to the reliability of the numerical process, we chose to verify whether the obtained numerical solution of the complete nonlinear problem tends in the case of a small amplitude loading, to the numerical solution of the linearized version of equations (6-7), i.e.

$$\begin{aligned} \frac{\partial^2 u}{\partial t^2} &= \frac{\partial^2 u}{\partial a^2} (\phi - K^2/\eta) - \frac{K}{\eta} \frac{\partial T}{\partial a} \\ \frac{\partial T}{\partial t} &= \frac{k\eta}{\rho T_1} \frac{\partial^2 T}{\partial a^2} - K \frac{\partial^2 u}{\partial a \partial t} \end{aligned} \tag{23}$$

together with the boundary conditions

$$\begin{aligned} m(0, t) &= \gamma f(t) \\ T(0, t) &= T_1 + \gamma f(t) \end{aligned} \quad (24)$$

where  $\gamma$  is a chosen parameter.

We chose for loading function  $f(t)$  the following smooth rising function:

$$f(t) = [t^2 H(t) - 2(t - \tau)^2 H(t - \tau) + (t - 2\tau)^2 H(t - 2\tau)]/2\tau^2. \quad (25)$$

This function rises from zero at  $t = 0$  up to 1 at  $t \geq 2\tau$ .

We expect the solutions of the nonlinear problem (6-7) and of the linear problem (23), both with the boundary conditions (24), to tend to each other for small  $\gamma$ . In Fig. 3 the displacement gradients  $m(a, t)$  are shown at  $a = 0.4$  with  $\tau = 0.1$  for the two cases of  $\gamma = 0.25$  and  $\gamma = 0.1$ . The fact that the nonlinear solution tends to the linear solution as  $\gamma$  becomes small is clearly seen. This indicates the proper behaviour of the nonlinear numerical procedure since for small applied inputs it yields solutions tending to those obtained directly from the linear case.

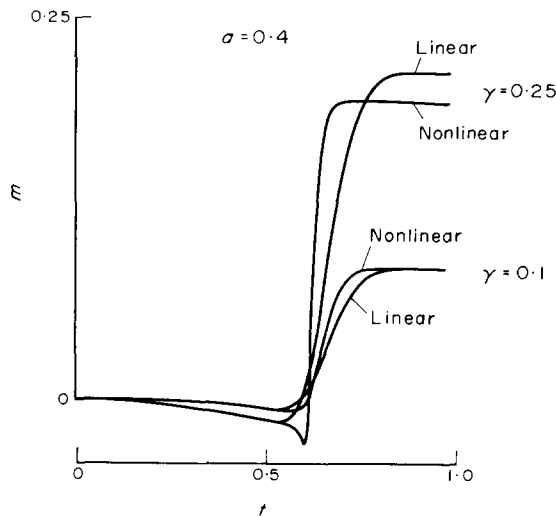


Fig. 3. The solution for the displacement gradients of the linear problem (23) and the nonlinear one (6-7), both with the boundary conditions (24) with  $\gamma = 0.25, 0.1$  at the station  $a = 0.4$ .

In the limiting case of zero conductivity ( $k = 0$ ) the governing equations of motion reduce to a purely hyperbolic one and the isentropic approximation ( $\partial S/\partial t = 0$ ) is obtained. In this case the difference equation (14) yields an entropy distribution which remains constantly zero throughout the body. It is known, Bland[10], that under an input of a monotonically decreasing continuous displacement gradient at the boundary, the purely mechanical problem with  $W = U(S = 0)$  and  $\partial^3 W/\partial m^3 > 0$ , admits a simple wave solution given by [7]

$$m(a, t) = \gamma f(t - a/c), \quad \gamma < 0. \quad (26)$$

In (26)  $f(t)$  is the time input (25) and  $c$  is the velocity of the acceleration waves given by

$$c = \left( \frac{\partial^2 W}{\partial m^2} / \rho \right)^{1/2}. \tag{27}$$

For the quadratic material (2) we obtain for the simple wave solution the condition that  $m > -1$ , together with the hyperbolicity condition  $1 + 3m + 1.5m^2 > 0$ .

The simple wave solution (26) provides an analytical check to the numerical scheme (11) in the special case of  $k = 0$ , and in Fig. 4 the analytical (26) and the numerical solutions

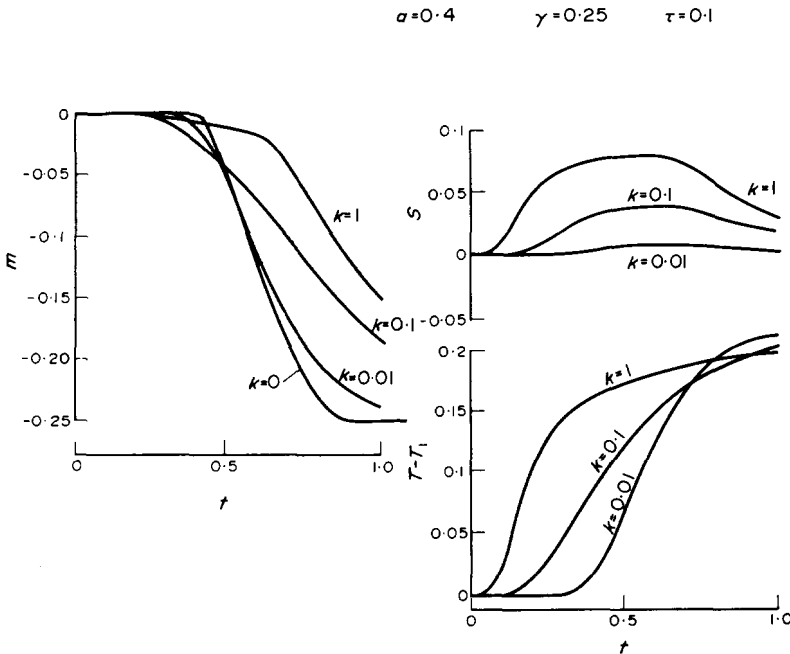


Fig. 4. Numerical solutions for the displacement gradient, the entropy and the temperature of the nonlinear problem with the boundary conditions (28) and  $\gamma = -0.25$ . The coefficients of conductivity  $k = 0, 0.01, 0.1, 1$ . The analytical solution (26) for the purely mechanical case ( $k = 0$ ) coincide with the numerical one.

are up to the scale of the plot indistinguishable. In Fig. 4 the results are shown for  $\gamma = -0.25$  and  $\tau = 0.1$ .

For the other non-zero values of  $k$  ( $k = 0.01, 0.1, 1$ ), numerical results for  $m, S$  and  $T$  are shown in Fig. 4 with the boundary conditions

$$\begin{aligned} m(0, t) &= \gamma f(t) \\ T(0, t) &= T_1 + K\gamma f(t)[1 + 0.5\gamma f(t)] \end{aligned} \tag{28}$$

which yield  $S = 0$  at  $a = 0$  for all  $t \geq 0$ .

Figure 4 exhibits the effect of the conductivity  $k$  on the various quantities considered. The departure of the solutions from the purely mechanical problem ( $k = 0$ ) is well seen.

## CONSTANT WAVE PROFILE

It was shown by Bland[10] that the mixed hyperbolic-parabolic equations of nonlinear thermoelasticity (6-7) admit solutions representing waves traveling rigidly without change of shape or of magnitude, that is waves propagating with a constant profile. For a smooth constant profile not containing shocks the equation that determines the variation of the displacement gradient across the wave, i.e. its variation from  $m = 0$  in the initial condition in which the medium is at rest, to its final value  $m = m^*$  is given by:

$$-\rho V \xi = \int k \frac{\partial T}{\partial m} / [U(m) - 0.5V^2 m^2] dm \quad (29)$$

where  $\xi = a - Vt$  and  $V$  is the constant velocity of the wave. Equation (29) yields an equation for  $m$  in terms of  $\xi$ . The variation of the entropy  $S$  across the wave is given by the equation[10]:  $\partial U / \partial m = V^2 m$  with  $m = m(\xi)$  obtained from (29). As to the constant velocity of propagation, it is obtained from the equations[10]

$$\left. \begin{aligned} \frac{\partial U}{\partial m} &= V^2 m \\ U &= 0.5V^2 m^2 \end{aligned} \right\} \text{ at } m = m^*. \quad (30)$$

Equations (29-30) furnish the complete solution for the constant wave profile (which is not including shocks) in a material whose internal energy  $U$  is given.

This analytical solution serves here as another check to the accuracy of the numerical scheme of the nonlinear problem with the appropriate initial and boundary conditions which correspond to the constant wave profile as will be described below.

In order to perform the integration in (29) in a closed form, we choose, following Bland[10] the material whose internal energy is given by

$$U = T_1 S + 0.5\phi m^2 - KmS + 0.5\eta S^2 + \theta m^3 \quad (31)$$

where  $\theta$  is another material parameter.

This yields for the constant wave profile according to (29-30) and for small  $m^*$  the following solution

$$\begin{aligned} m(\xi) &= 0.5m^*[1 - \tanh \alpha\xi], & \alpha &= 3\rho V\theta T_1 m^*/2kK^2 \\ S(\xi) &= -3\theta m(m^* - m)/K + 0(m^*)^3 \\ T(\xi) &= T_1 - Km + \eta S \end{aligned} \quad (32)$$

with

$$V = \phi + 1.5\theta m^*/\phi.$$

The displacement  $u(\xi)$  is obtained by a direct integration

$$u(\xi) = 0.5m^* \left[ \xi - \frac{1}{\alpha} \log \cosh \alpha\xi \right]. \quad (33)$$

On the other hand the equations of motion which correspond to (31) are given according to (3) by:

$$\begin{aligned} \frac{\partial^2 u}{\partial t^2} &= \left( \phi - \frac{K^2}{\eta} + 6\theta \frac{\partial u}{\partial a} \right) \frac{\partial^2 u}{\partial a^2} - \frac{K}{\eta} \frac{\partial T}{\partial a} \\ T \frac{\partial T}{\partial t} &= \frac{k\eta}{\rho} \frac{\partial^2 T}{\partial a^2} - KT \frac{\partial^2 u}{\partial a \partial t}. \end{aligned} \quad (34)$$

These equations can be solved numerically as described previously together with the following initial and boundary conditions which correspond to the constant wave profile whose analytical solution is given by (32):

$$\left. \begin{aligned} u(a, 0) &= u(\xi) \\ \frac{\partial u}{\partial t} &= -V \frac{\partial u}{\partial \xi} \end{aligned} \right\} \text{ at } t = 0 \tag{35}$$

$$\left. \begin{aligned} m(0, t) &= m(\xi) \\ T(0, t) &= T(\xi) \end{aligned} \right\} \text{ at } a = 0 \tag{36}$$

and

$$\left. \begin{aligned} u(a_1, t) &= u(\xi) \\ T(a_1, t) &= T(\xi) \end{aligned} \right\} \text{ at } a = a_1 = N \Delta a. \tag{37}$$

The boundary conditions at  $a_1 = N \Delta a$  are necessary since the constant wave profile (32) tends to zero at very large values of  $a$  for our time range of interest  $0 \leq t \leq 1$  for which the numerical solution is produced.

In Fig. 5 the displacement gradients obtained numerically are shown with  $\theta = 1$ ,  $m^* = \pm 0.1$

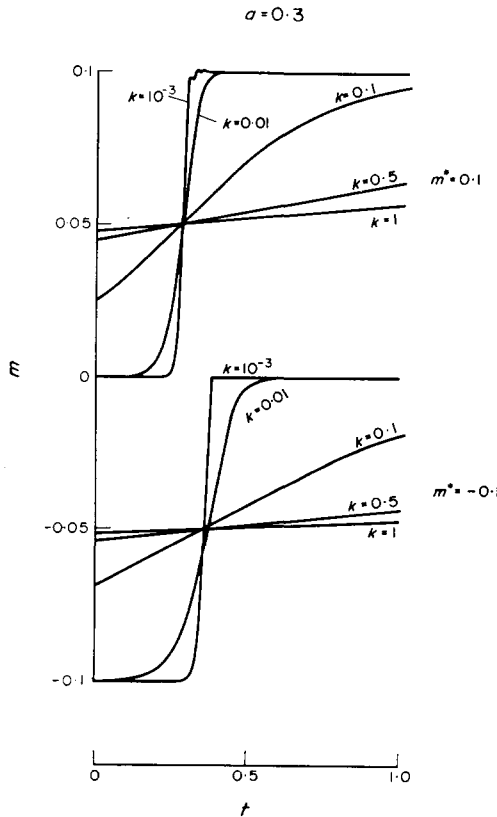


Fig. 5. Displacement gradients of the constant waves profile with  $m^* = 0.1, -0.1$  and  $k = 1, 0.5, 0.1, 0.01, 0.001$  at station  $a = 0.3$ .

at  $a = 0.3$  for the following values of conductivity  $k = 1, 0.5, 0.1, 0.01, 0.001$ . Note that for a non-conductive material ( $k = 0$ ) the wave profile is given by  $m(a, t) = H(a - Vt)$ . The correspondence between the analytical and the numerical solutions is excellent as it is shown in Table 1 where the displacement gradients are given for the case of  $m^* = 0.1, k = 0.1$  at  $a = 0.3$  for  $0 \leq t \leq 1$ .

Table 1. Constant wave profile solution: a comparison between analytical and numerical solutions for the displacement gradient

$t$	Analytical	Numerical
0.05	$3.022 \times 10^{-2}$	$3.022 \times 10^{-2}$
0.10	3.456	3.455
0.15	3.918	3.917
0.20	4.399	4.401
0.25	4.892	4.903
0.30	5.387	5.413
0.35	5.875	5.901
0.40	6.346	6.388
0.45	6.793	6.857
0.50	7.209	7.289
0.55	7.590	7.679
0.60	7.934	8.027
0.65	8.240	8.332
0.70	8.510	8.597
0.75	8.744	8.824
0.80	8.946	9.018
0.85	9.119	9.182
0.90	9.266	9.322
0.95	9.390	9.441
1.00	9.494	9.540

$$m^* = 0.1, k = 0.1, a = 0.3.$$

The smearing effect of the finite conductivity on the propagating wave is well seen in Fig. 5. Indeed it is shown in [10] that the width of the constant wave profile is roughly proportional to the conductivity for small amplitudes.

#### SHOCKS IN A CONDUCTING HALF-SPACE

We deal now with solutions of thermoelastic wave propagation in a half-space which contain shocks. We choose to deal with the following boundary conditions:

$$\begin{aligned} m(0, t) &= 0.5H(t) \\ T(0, t) &= T_1. \end{aligned} \quad (38)$$

The equations of motion are given by (6-7) and their corresponding numerical scheme is given by (11-14). The initial conditions are given by (8).

It is known[10] that in the case of a nonconducting solid ( $k = 0$ ), the disturbance due to a step input of strength  $m$  on the boundary propagates as a shock with a velocity given by:

$$V = \left( \frac{\partial U}{\partial m} / m \right)^{1/2} \quad (39)$$

without a change in its strength. The solutions for the conductive cases will therefore exhibit the smearing effect of the finite conductivity on the propagating shock.

In Fig. 6 the solutions at  $a = 0.5$  for displacement gradient  $m$ , the particle velocity  $v = \partial u / \partial t$ , the entropy  $S$  and the temperature  $T - T_1$  are shown for  $k = 1, 0.1, 0.01$  and the smoothing effect is clearly seen.

These shock solutions must obey the momentum, energy, entropy and compatibility conditions which must hold across the shock. In our case these conditions can be combined and shown to be equivalently given by[10]:

$$\left[ \frac{\partial U}{\partial m} \right] = V^2[m] \tag{40}$$

$$VT[S] \geq V[U] + 0.5V[v^2] + \left[ v \frac{\partial U}{\partial m} \right] \tag{41}$$

$$[v] + V[m] = 0 \tag{42}$$

where  $[f]$  denotes the change of  $f$  across the shock. The fulfillment of these jump conditions across the shock in the numerical solutions clearly indicate the reliability of the finite difference scheme in handling discontinuous solutions also.

Let us illustrate the fulfillment of these conditions for the case of  $k = 1$  in Fig. 6. In this case we obtain by a direct measuring of the various quantities in the graph that  $[m] = 0.255$ ,  $[S] = 0.152$ ,  $[v] = -0.245$  and  $V = 0.96$ . Then  $[\partial U / \partial m] = 0.217$  and  $V^2[m] = 0.234$  showing that (40) is well satisfied. Moreover the left and right hand sides of (41) yield 0.106, showing that up to the accuracy of the measuring procedure (41) holds as an equality. It is worthwhile to mention that for lower values of  $k$  for which the jump conditions (40-42)

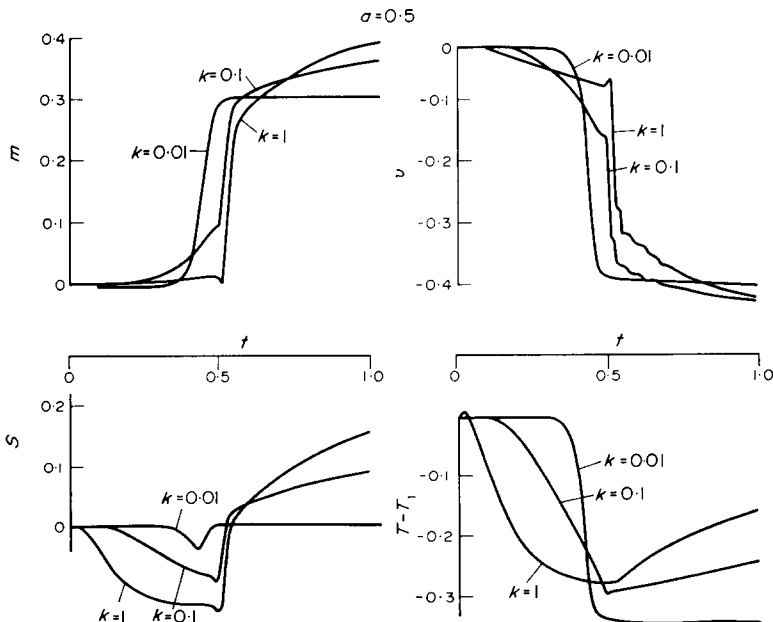


Fig. 6. Displacement gradients, particle velocities, entropies and temperatures of the non-linear problem with the boundary conditions (38) are shown for  $k = 1, 0.1, 0.01$  at station  $a = 0.5$ .

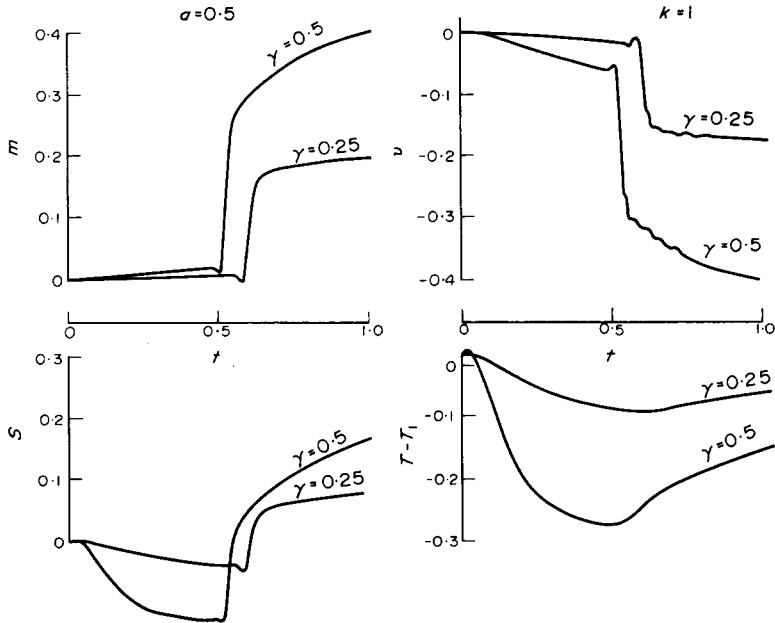


Fig. 7. Same as Fig. 6 for  $k = 1$  and  $\gamma = 0.5, 0.25$ .

were checked as well, we obtained strict inequalities for (41). With regard to the compatibility condition (42), we have  $V[m] = 0.245$  showing excellent satisfaction of (42). We conclude therefore that the numerical solution yields the right jumps across the shock according to the above conditions.

In [10] it is proved that the temperature  $T$  is continuous across the shock, i.e.  $[T] = 0$ . This is indeed well seen in the various curves of  $T$  in Fig. 6. We may note also that even in the case of small conductivity  $k = 0.01$ , still a significant jump in  $S$  is obtained indicating that the purely mechanical solution ( $k = 0$ ) must be considered as a strictly limiting case.

In Fig. 7 we compare the solutions which correspond to the boundary conditions  $m(0, t) = 0.5H(t), 0.25H(t)$  respectively. The observation point is at  $a = 0.5$  and the coefficient of conductivity  $k = 1$ . Note that in the stronger jump with  $0.5H(t)$  we obtain larger propagation velocity  $V$  as compared with the smaller jump  $0.25H(t)$ . This is again in accordance with the results of Bland[10].

## CONCLUSION

A numerical scheme is presented for the solution of one-dimensional coupled nonlinear thermoelastic equations. The reliability of the method is checked and demonstrated by comparison with analytical solutions which can be obtained in some special cases. It is also shown that cases with shock waves are successfully treated. The method can be applied and used in other unsolved nonlinear thermoelastic wave propagation problems.

## REFERENCES

1. B.-T. Chu, Finite amplitude waves in incompressible perfectly elastic materials. *J. Mech. Phys. Solids* **12**, 45-57 (1964).
2. W. D. Collins, One-dimensional wave propagation in incompressible elastic materials. *Quart. J. Mech. appl. Math.* **19**, 259-328 (1966).

3. D. P. Reddy and J. D. Achenbach, Simple waves and shock waves in a thin prestressed elastic rod. *ZAMP* **19**, 473–485 (1968).
4. J. D. Achenbach and D. P. Reddy, Shear waves in finite strain generated at the surface of a viscoelastic half-space. *Int. J. Engng. Sci.* **5**, 527–539 (1967).
5. J. Lubliner and R. J. Green, Shock-wave propagation in instantaneously nonlinear materials. *J. de Mec.* **9**, 507–522 (1970).
6. J. P. Vogt and R. A. Schapery, Uniaxial shock wave propagation in a viscoelastic material. *Int. J. Solids Struct.* **7**, 505–521 (1971).
7. J. Aboudi and Y. Benveniste, One dimensional finite amplitude wave propagation in a compressible elastic half-space. *Int. J. Solids Struct.* **9**, 363–378 (1973).
8. B. A. Boley and I. S. Tolins, Transient coupled thermoelastic boundary value problems in the half-space. *J. appl. Mech.* **29**, 637–646 (1962).
9. A. I. Soler and M. A. Brull, On the solution to transient coupled thermoelastic problems by perturbation techniques. *J. appl. Mech.* **32**, 389–399 (1965).
10. D. R. Bland, *Nonlinear Dynamic Elasticity*. Blaisdell (1969).
11. R. E. Craine, The quasi-transverse constant profile wave in finite elasticity. *Quart. J. Mech. appl. Math.* **23**, 17–34 (1970).
12. E. Sternberg and J. G. Chakravorty, On inertia effects in a transient thermoelastic problem. *J. appl. Mech.* **26**, 503–509 (1959).
13. O. W. Dillon, Thermoelasticity when the material coupling parameter equals unity. *J. appl. Mech.* **32**, 378–382 (1965).
14. R. D. Richtmyer and K. W. Morton, *Difference Methods for Initial-Value Problems*, 2nd Edn. Interscience (1967).

**Абстракт** — Исследуется распространение конечной волны в нелинейно термоупругом полупространстве. Поверхность полупространства подвержена действию нагрузки, зависящей от времени и нормальной, механической. Получается решение на основе численного метода, который дает точные результаты. В качестве специальных случаев, получаются линейные, динамические, термоупругие задачи. Проверяется точность результатов, путем сравнения с некоторыми известными аналитическими решениями, которые можно определить для некоторых специальных случаев, как линейных так и нелинейных задач. Указывается, далее, что для случаев, где решение содержит скачки, численные результаты удовлетворяют необходимым условиям разрыва функции, которые-то нужны удерживаться поперёк таких точек разрыва.